Supplementary Information

Previous QM works. Supplementary Table S1 summarizes previous QM studies published to date, describing HB dimer interactions at non-optimal geometries, with the aim of characterizing variation in ΔE with angular components. Most of the previous studies considered only one angular component. Others addressed multiple angular components separately (Morozov et al.[13,67] and Řezáč et al.[68]). We could find only a single study in which two angular components were addressed simultaneously for the same target site (Lamas et al.[69]).

Supplementary Table S1 Previous QM studies of HB directionality which considered interaction energies at non-optimal geometries (ranked by publication year)

Ref	Year	Acceptors	Donors	Level of theory	Geometric parameters [a]
Lamas et al.[69]	1992	N(sp^2)	-	HF/3-21G	$f(\theta,\phi)$
Platts et al.[70]	1996	O(sp^2,sp^3) S(sp^2,sp^3)	-	multipole electrostatics [b]	$f(\phi)$
Allen et al.[71]	1997	NO_2	-	IMPT/6-31G**	$f(\phi)$
Morozov et al.[13,67]	2004	formamide	formamide	PBE96/aug-cc-pVDZ	$f(\theta)$, $f(\phi)$
Nanda et al.[72]	2007	-	CH(aromatic)	B3LYP/6-11++G**	$f(\phi)$
Wood et al.[20]	2008	O(sp^2) S(sp^2)	-	IMPT/6-31G**	$f(\phi)$
Wood et al.[73]	2009	-	OH(sp^3) CH(sp,sp^2)	IMPT/6-31G**	$f(\phi)$
Choi et al.[74]	2009	N-methylacetamide	N-methylacetamide	B3LYP/6-311G**	$f(\phi)$
Choi et al.[75]	2010	O(sp^2)	NH(sp^2) OH(sp^3)	B3LYP/6-311G**	$f(\phi)$
Řezáč et al.[68]	2011	10	10	CCSD(t)/CBS	$f(\phi)$, $f(\theta)$
Lu et al.[76]	2011	O(sp^2,sp^3) N(sp,sp^2,sp^3) S(sp^2,sp^3)	-	B3LYP-D3/aug-cc-pVDZ	$f(\phi)$
Tafipolsky et al.[77]	2016	water	-	DFT-SAPT/aug-cc-pVQZ	$f(\phi)$
Mondal et al.[78]	2017	O(sp^2)	-	M06-2X/6-311+G*	$f(\phi)$

[a] θ and ϕ values as depicted in Fig. 5
[b] multipoles were derived from MP2 level of theory.

Level of theory validation. Given the large number of independent computations to be performed, we employed the B3LYP density functional with the cc-pVDZ basis set and D3 dispersion corrections with BJ-damping. B3LYP is known to systematically underestimate absolute interaction energies [79], but numerous previously reported works show that it provides accurate ranking of relative HB strengths [80–82], which is adequate for the scope of this work. As a validation, we performed multiple tests using MP2/aug-cc-pVTZ on a small sample of compounds (using the counterpoise correction), and compared the results obtained with the two levels of theory, assessing the impact of the different protocols on the error in both HB strengths and anisotropy profiles.

Accuracy of HB strengths. We compared the values of ΔE_{opt} of dimer geometries fully minimized with B3LYP-D3BJ/cc-pVDZ, B3LYP/cc-pVTZ and MP2/aug-cc-pVTZ levels of theory. A small subset of 33 dimers was used for this comparison: dimethylamine **9** – HCN **51**, HCN **19** – dimethylamine **89**, HCN **19** – dimethyl ether **64**, HCN **19** – dimethyl sulfide **60**, HCN **19** – furan **41**, HCN **19** – HCN **51**, HCN **19** – methylamine **88**, HCN **19** – methanol **66**, HCN **19** – methanethiol**47**, HCN **19** – water **65**, methanol **15** – HCN **51**, methanol **15** – methylamine **88**, methanol **15** – methanol **66**, methanol **15** – methanethiol **47**, methanol **15** – water **65**, pyrrole **18** – HCN **51**, pyrrole **18** – water **65**, methanethiol **6** – HCN **51**, methanethiol **6** – methylamine **88**, methanethiol **6** – methanethiol **47**, methanethiol **6** – water **65**, water **13** – dimethylamine **89**, water **13** – dimethyl ether **64**, water **13** – dimethyl sulfide **60**, water **13** – furan **41**, water **13** – HCN **51**, water **13** – methylamine **88**, water **13** – methanol **66**, water **13** – pyridine **80**, water **13** – methanethiol **47**, water **13** – trimethylamine **86** and water **13** – water **65**. Optimizations were performed with the counterpoise correction. Four of the dimers showed negative frequencies but were considered nevertheless. The energy difference between B3LYP-D3BJ/cc-pVDZ and MP2/aug-cc-pVTZ is systematic and within about 1.0 kcal/mol, (Fig. S1), in agreement with previous studies.[79] The use of dispersion corrections seems to fix the systematic underestimation of absolute interaction energies by B3LYP. We consider that there is satisfactory agreement between B3LYP-D3BJ and MP2/aug-cc-pVTZ.

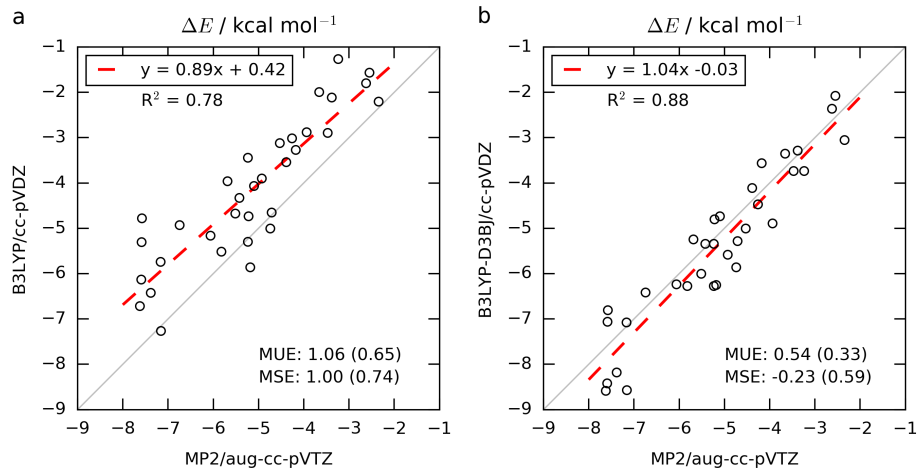

Supplementary Figure S1 Interaction energies of 33 dimers at the MP2/aug-cc-pVTZ and B3LYP/cc-pVDZ levels of theory, excluding (a) or including (b) dispersion corrections. Each dimer was fully optimized with each level of theory using the counterpoise correction. The red dashed line is a linear fit. The gray line is the identity line. The mean signed error (MSE) and the mean unsigned error (MUE) were calculated for the raw ΔE values, i.e., not using the linearly fitted data. The values in brackets are standard deviations.

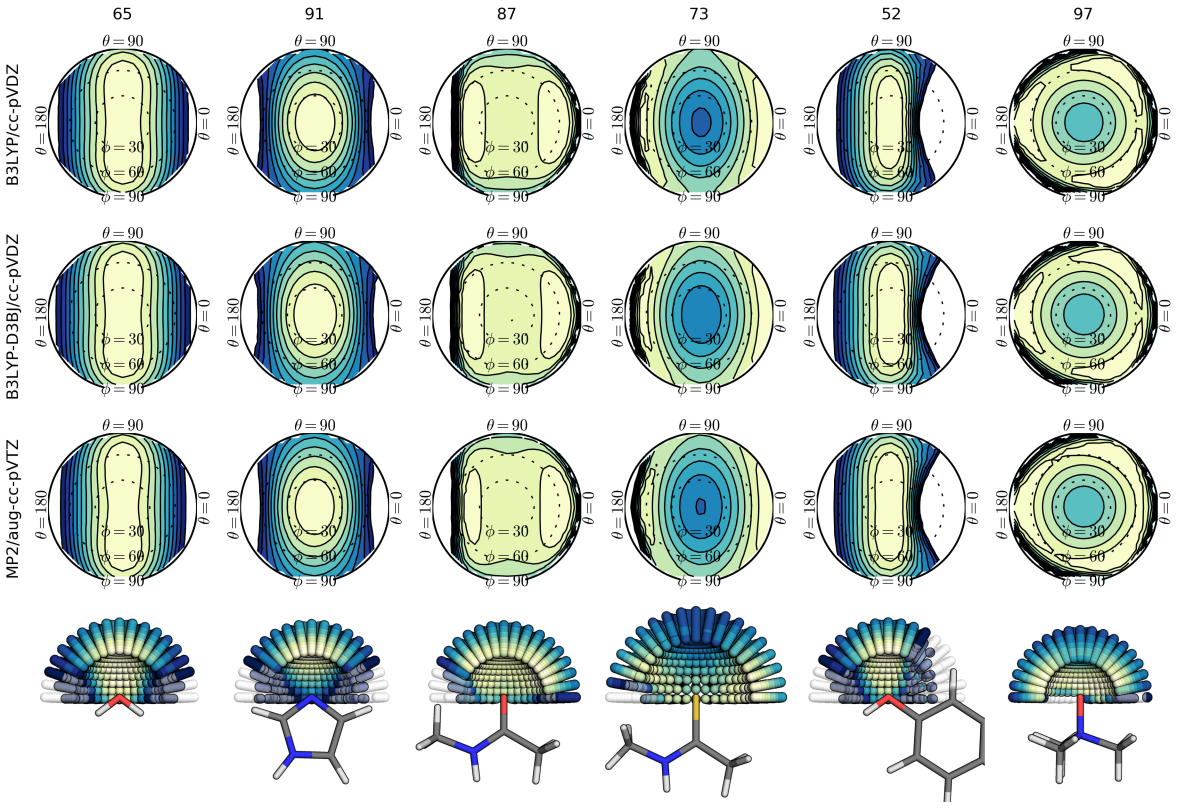

Supplementary Figure S2 Directionality profiles of acceptor sites calculated with different levels of theory.

Accuracy of anisotropy profiles. To assess the quality of directionality profiles calculated with B3LYP-D3BJ/cc-pVDZ we used MP2/aug-cc-pVTZ to compute domes for donor and acceptor sites of water (**13**, **65**), imidazole (**23**, **91**), methyl-acetamide (**17**, **87**), methyl-thioacetamide (not numbered as donor; compound **73** as acceptor), phenol (**25**, **52**), and trimethylamine-N-oxide (**97**). Results are summarized in Supplementary Table S2, Supplementary Figures S2 and S3. The equal area projections obtained with dispersion corrected B3LYP and MP2 are nearly indistinguishable.

Supplementary Table S2 Directionality indexes calculated with MP2/aug-cc-pVTZ and B3LYP/cc-pVDZ. HF probes acceptor sites. HCN probes donor sites

target type	probe	target	MP2/aug-cc-PVTZ		B3LYP-D3BJ/cc-pVDZ		B3LYP/cc-pVDZ	
			$\Delta E_{opt(HF)}$	$D_{[\mathrm{HF}]}$	$\Delta E_{opt(HF)}$	$D_{[\mathrm{HF}]}$	$\Delta E_{opt(HF)}$	$D_{[\mathrm{HF}]}$
acceptor	HF	water **65**	-8.3	0.34	-9.3	0.33	-8.7	0.34
acceptor	HF	phenol **52**	-7.3	0.37	-7.3	0.38	-6.2	0.42
acceptor	HF	imidazole **91**	-13.4	0.43	-12.7	0.42	-11.6	0.45
acceptor	HF	*N*-methyl-acetamide **87**	-11.9	0.21	-11.6	0.19	-10.4	0.21
acceptor	HF	*N*-methyl-thioacetamide **73**	-9.2	0.38	-9.7	0.34	-8.3	0.36
acceptor	HF	trimethylamine-N-oxide **97**	-19.1	0.25	-19.0	0.25	-17.2	0.25
			$\Delta E_{opt(HCN)}$	$D_{[\mathrm{HCN}]}$	$\Delta E_{opt(HCN)}$	$D_{[\mathrm{HCN}]}$	$\Delta E_{opt(HCN)}$	$D_{[\mathrm{HCN}]}$
donor	HCN	water **13**	-3.9	0.49	-3.5	0.46	-2.9	0.48
donor	HCN	phenol **25**	-5.7	0.49	-5.7	0.49	-4.4	0.54
donor	HCN	imidazole **23**	-5.7	0.33	-5.4	0.37	-4.4	0.46
donor	HCN	*N*-methyl-acetamide **17**	-4.7	0.37	-4.4	0.39	-3.3	0.48
donor	HCN	*N*-methyl-thioacetamide	-5.6	0.35	-5.3	0.36	-4.1	0.45

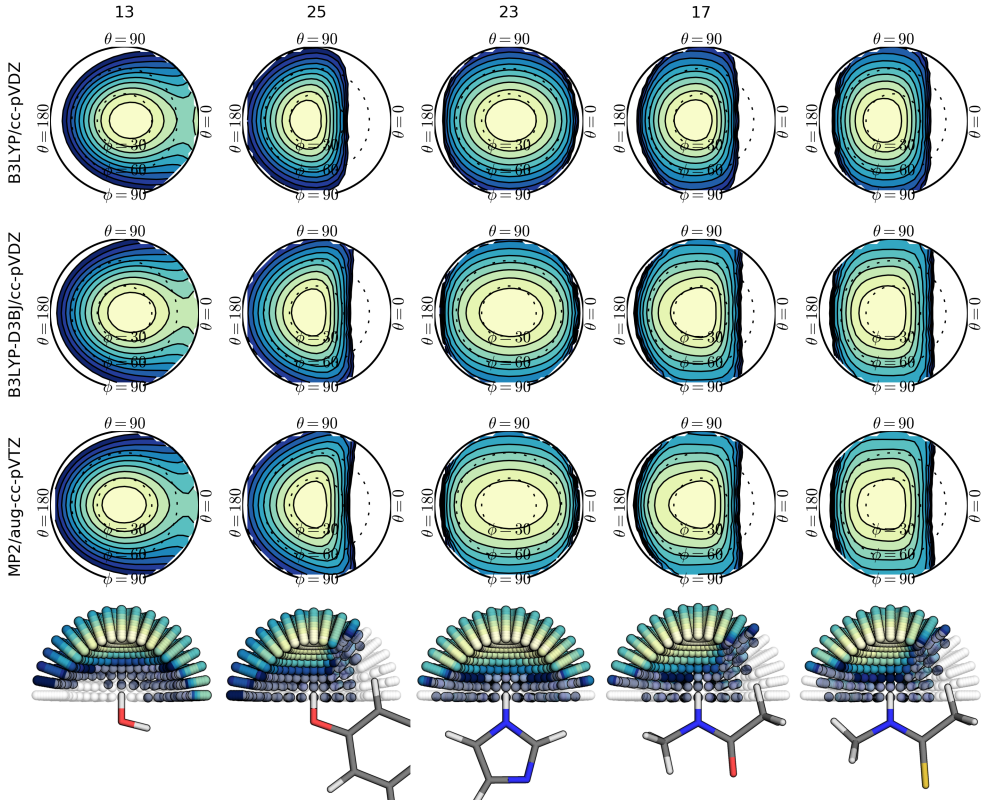

Supplementary Figure S3 Directionality profiles of donor sites calculated with different levels of theory.

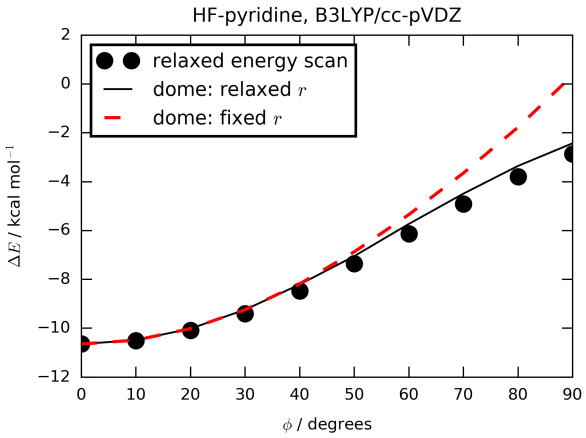

Supplementary Figure S4 Directionality profiles obtained using the rigid monomer approach compared to a relaxed energy scan (in which bond lengths and angles are allowed to relax).

Internal geometry constraints. When calculating domes, we generated input geometries in an automated fashion and performed a single point energy evaluations for each geometry. During these calculations structures were not allowed to relax, specifically bond lengths and bond angles, in order to preserve the intended (r, ϕ, θ) values. This could create artificially high energies when angles are far from the optimum, and repulsions occur. To assess the effect of these restraints on calculated energies, we performed a relaxed energy scan along the ϕ angle of the HF-pyridine dimer (Fig. S4, *black circles*), and compared it with the energy profile obtained using rigid monomers at fixed distance (Fig. S4, *red dashed line*). The distance between the red dashed line and the black circles is the energy error in the domes if fixed r were used. When the distance between the donor hydrogen and the acceptor atom is allowed to relax (Fig. S4, black solid line), negligible differences are found. Therefore the r distance scan was included in the calculation of domes.

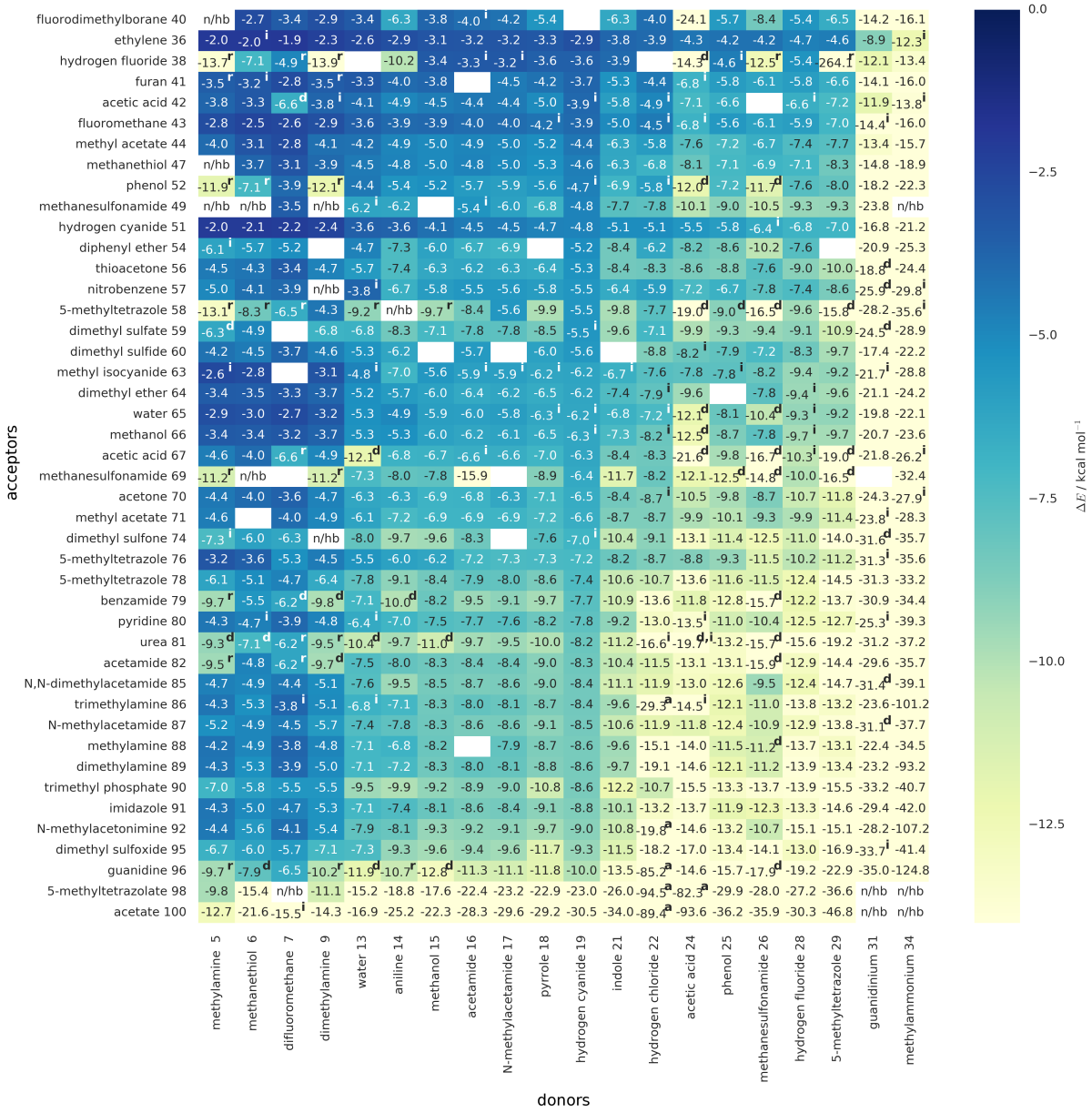

Supplementary Figure S5 Interaction energies between donor (*columns*) and acceptor (*rows*) groups, ranked by their interaction energy with the reference probe HCN (**51** and **19**, respectively). By visual inspection of the optimized geometries, as well as frequency calculations, we identified and annotated some dimers with the following issues: *i* imaginary frequencies (optimized to transition state); *d* multi-furcated HB; *r* inversion of donor/acceptor roles; *a* dissociation of acidic proton; *n/hb* not a hydrogen bond between the atoms of interest or clearly far from an ideal HB geometry. Due to the large number of dimers, we don't guarantee that dimers without annotations are free of these or other issues.

Supplementary Table S3 Variations of directionality values calculated with MP2 for imidazole, acetone, and dymethyl sulfoxide using acetylene **10** ($D_{[acetylene]}$) , water **13** ($D_{[water]}$), HCN **19** ($D_{[HCN]}$), and HF **28** probes ($D_{[HF]}$)

	$D_{[acetylene]}$	$D_{[water]}$	$D_{[HCN]}$	$D_{[HF]}$
imidazole **91**	0.32	0.35	0.34	0.43
acetone **70**	0.18	0.23	0.19	0.27
dymethyl sulfoxide **95**	0.16	0.24	0.14	0.19

Supplementary Table S4 Interaction energies ΔE_{opt} between imidazole, acetone and dymethyl sulfoxide and four donors: acetylene **10**, water **13**, HCN **19** and HF **28**. The level of theory is MP2/aug-cc-pVTZ with counterpoise correction.

	$\Delta E_{opt[acetylene]}$	$\Delta E_{opt[water]}$	$\Delta E_{opt[HCN]}$	$\Delta E_{opt[HF]}$
imidazole **91**	-4.3	-7.2	-8.1	-13.4
acetone **70**	-3.4	-5.9	-6.1	-10.0
dymethyl sulfoxide **95**	-4.6	-8.4	-8.0	-13.0

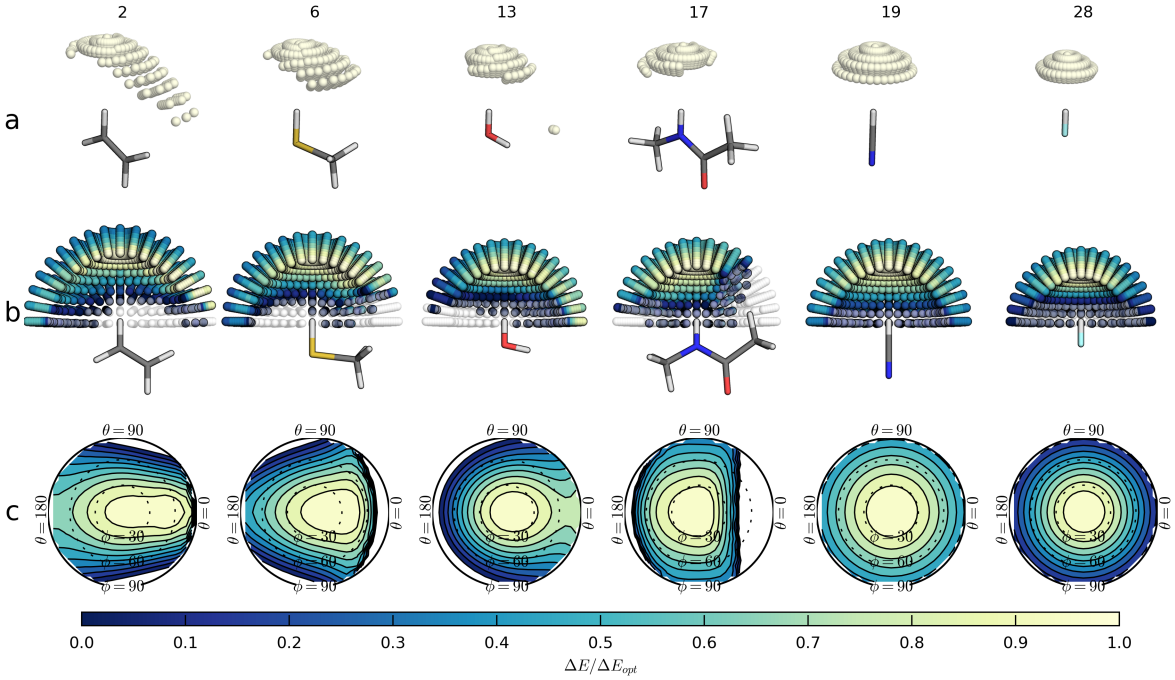

Supplementary Figure S6 Directionality of donors.

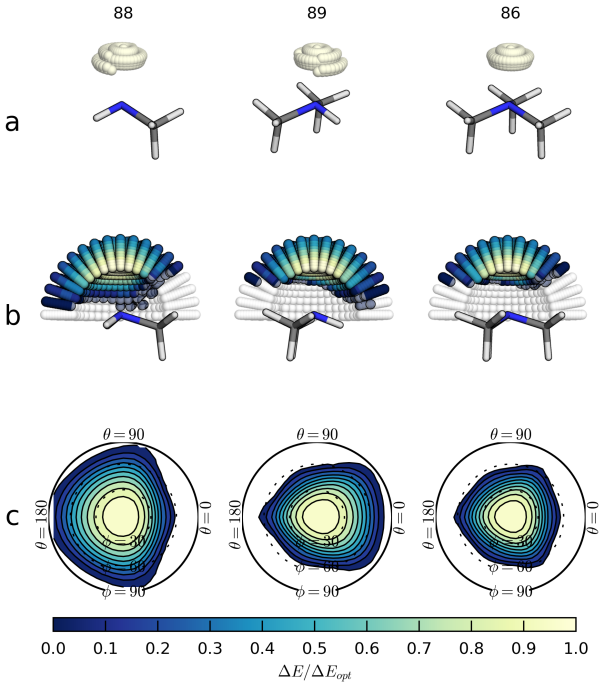

Supplementary Figure S7 Directionality of amines.

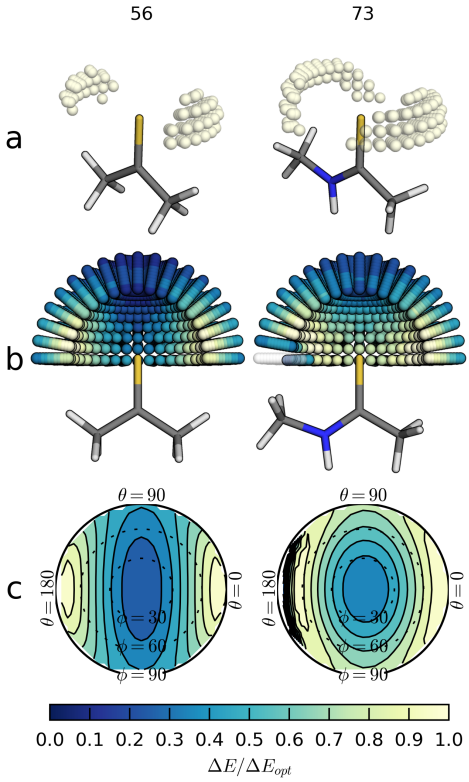

Supplementary Figure S8 Directionality of sp^2 sulfur.

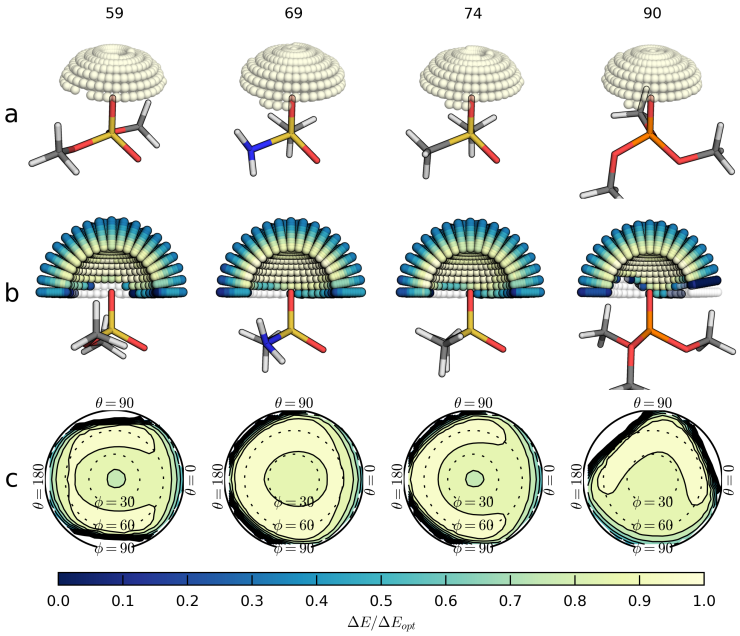

Supplementary Figure S9 Directionality of oxygen bound to sulfur or phosphate.

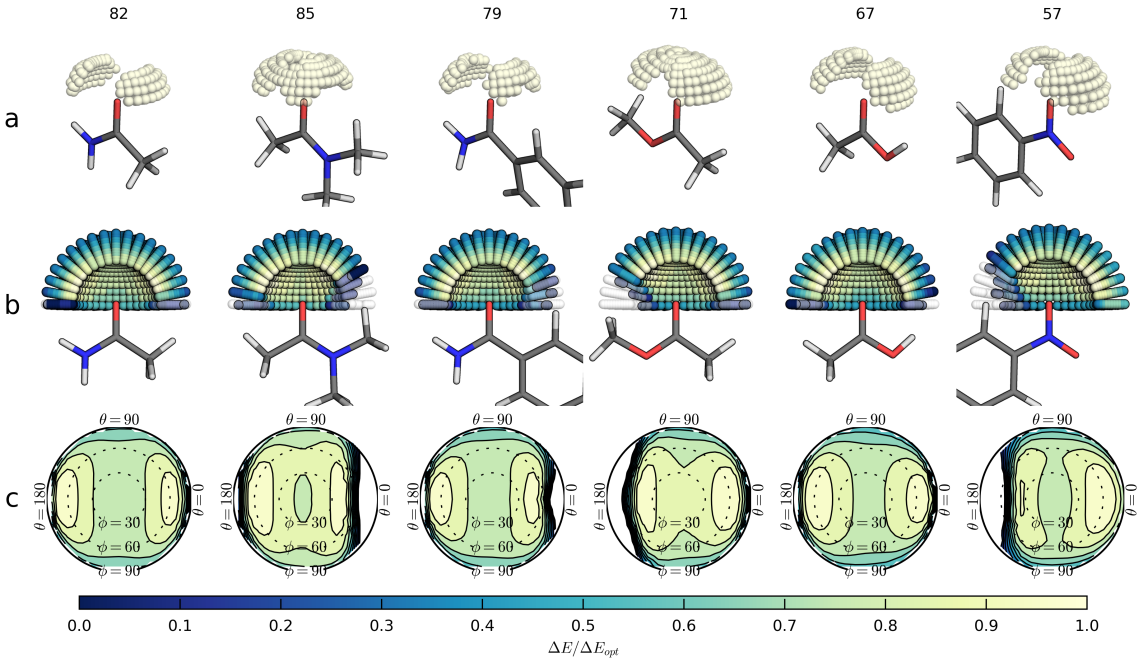

Supplementary Figure S10 Directionality of various sp^2 oxygens.

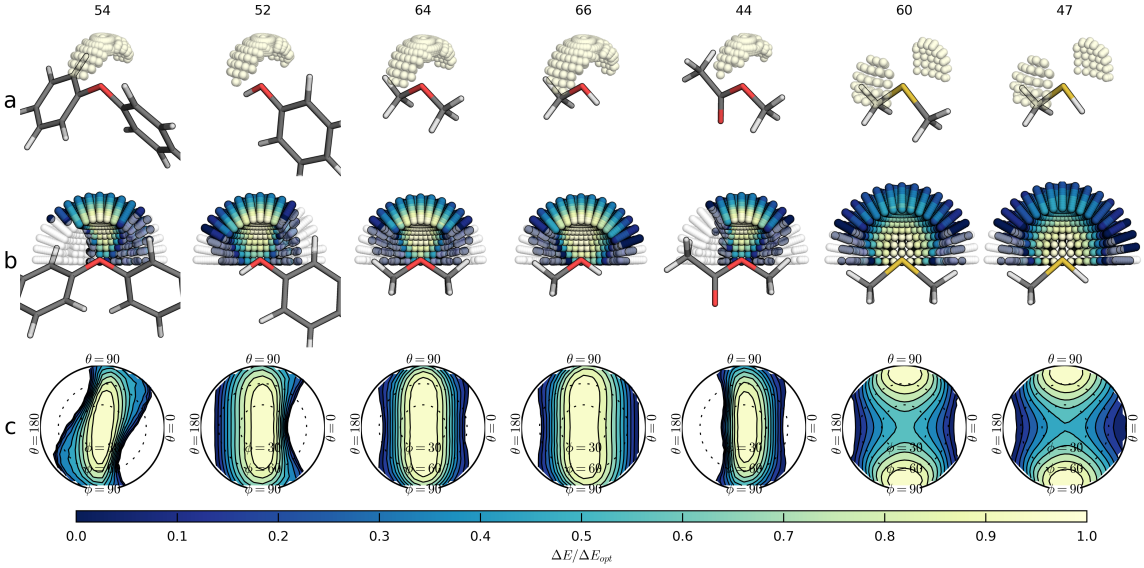

Supplementary Figure S11 Directionality of various sp^3 oxygen and sulfur groups.

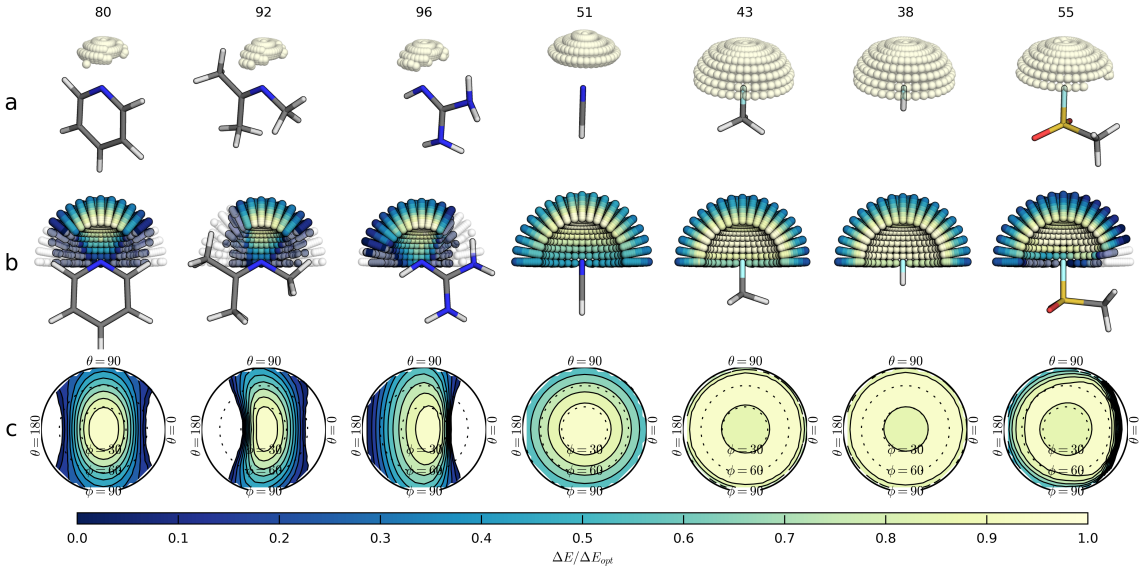

Supplementary Figure S12 Directionality of other acceptors.

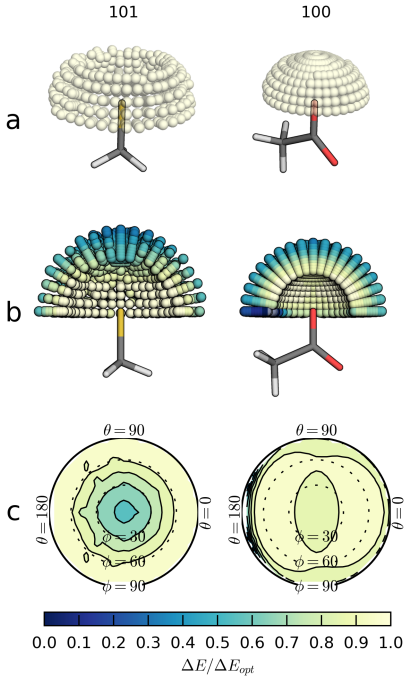

Supplementary Figure S13 Directionality of anions.

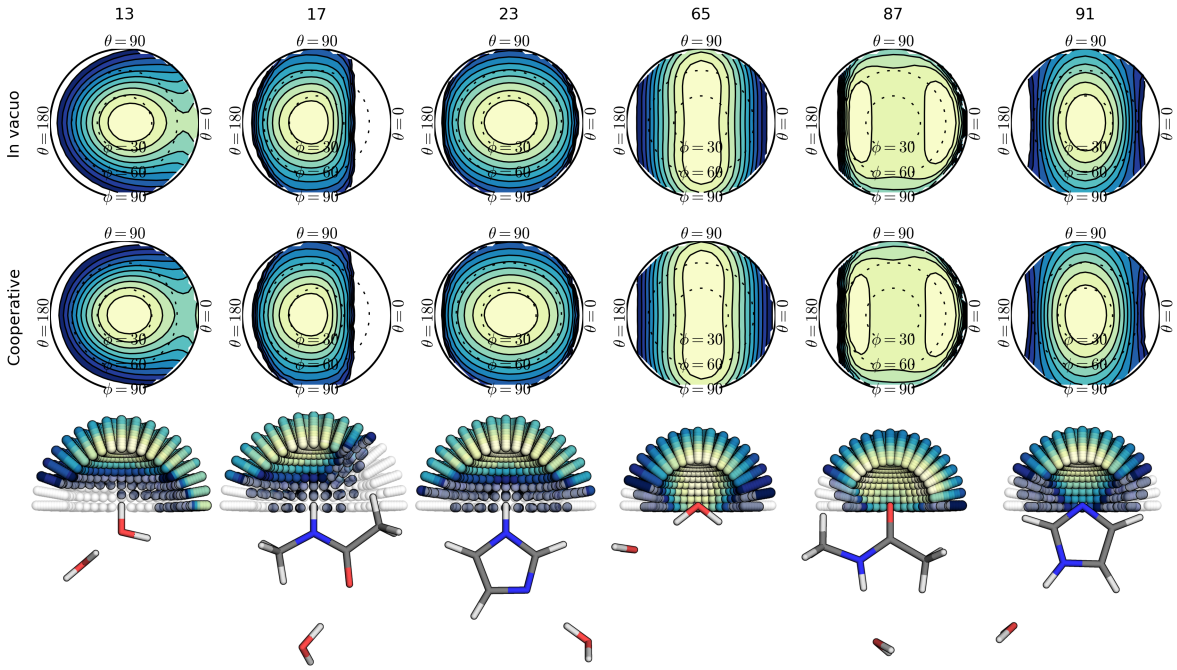

Supplementary Figure S14 Directionality profiles without (**a**) and with (**b**) cooperative effects. An explicit water molecule was added to create a HB network involving the added water molecule, the target molecule under study, and the probe. The B3LYP/cc-pVDZ level of theory was used.

Supplementary Table S5 Directionality and strength in cooperative HBs: acceptor sites. The level of theory is B3LYP/cc-pVDZ.

	In vacuo		Cooperative	
	$\Delta E_{\mathrm{opt[HF]}}$	$D_{\mathrm{[HF]}}$	$\Delta E_{\mathrm{wat[HF]}}$	$D_{\mathrm{[HF]}}$
water **65**	-8.7	0.34	-10.9	0.31
N-methylacetamide **87**	-10.4	0.21	-10.9	0.21
imidazole **91**	-11.6	0.45	-13.4	0.42

Supplementary Table S6 Directionality and strength in cooperative HBs: donor sites. The level of theory is B3LYP/cc-pVDZ.

	In vacuo		Cooperative	
	$\Delta E_{\mathrm{opt[HCN]}}$	$D_{\mathrm{[HCN]}}$	$\Delta E_{\mathrm{wat[HCN]}}$	$D_{\mathrm{[HCN]}}$
water **13**	-3.2	0.47	-3.9	0.48
N-methylacetamide **17**	-3.6	0.46	-3.7	0.47
imidazole **23**	-4.8	0.43	-5.2	0.43